Earthquake Engineering, Tenth World Conference © 1992 Balkema, Rotterdam. ISBN 90 5410 060 5

Performance of buried pipelines, subjected to fault movement

E.A.Vougioukas & P.G.Carydis
National Technical University, Athens, Greece

ABSTRACT: Earthquakes have demonstrated the vulnerability of buried pipelines in cases of permanent soil deformations rather than in ground shaking. A model is proposed, dealing with the analysis of the performance of shallow buried pipelines, subjected to fault movement. An analysis procedure is presented, applicable to both horizontal and vertical fault movement, either for strike slip or reverse strike slip fault. Results of the analysis, concerning the influence of parameters such as angle of pipe crossing the fault, geometric characteristics of pipe etc, are presented and commented. The ductility demands for the pipelines to resist large fault movement have been calculated.

1 INTRODUCTION

Buried pipelines play an important role in civil life. Their damage could lead to loss of vital services, communication, transportation etc and could sometimes result to a major disaster. Buried structures subject to earthquakes are particularly infuenced by the deformation of the ground surrounding them. Deformation of the ground can be caused by abrupt displacement of an active fault, liquefaction, landslides and travelling seismic waves. Among them, fault movement is major cause for pipelines' damage after severe earthquakes. This was reported after many significant earthquakes in the last years.

Though the important role of buried pipelines in human life is worldwide recognized, Earthquake Regulations do not include much concerning pipelines' earthquake resistant analysis and design, compared to what is included about other types of structures. However, a pipeline system is generally built up over a large territory and is subject to a variety of possible earthquake induced hazards; especially in the case of regions with high seismisity, e.g. Greece, it is almost impossible for a major pipeline not to cross a number of active faults!

In such cases, the response of buried pipelines to fault movement is an important part of lifeline earthquake engineering and its investigation is in line with the modern aspects on the subject.

2 FORMULATION OF THE PROBLEM

The model used in the present analysis, for the case of vertical fault movement, is shown in Figure 1 (side view).

A fault movement causes the relative displacement (ΔV) of the soil surrounding the pipeline. As the soil at the left hand side moves downwards, the relative motion of the pipeline is upwards and the reaction to this movement is due to the uplift reaction of the soil. As the soil at the right hand side moves upwards, the relative motion of the pipeline is downwards and the reaction to this movement is due to the bearing capacity reaction of the soil. The total relative motion of the pipeline consists of both parts:

$$\Delta V = \Delta V_1 + \Delta V_2$$

The model is assumed to consist of two curved segments (AB_1 and AB_2), each one of constant curvature joined at point A, near the transition zone, and two semi-infinite segments on elastic foundation, away from the transition zone. This assumption of an elastic foundation is permitted by the small value of soil deformations on the semi-infinite segments of the pipeline.

The described model includes also the assumption that point A is the first point where a plastic hinge of the pipeline will occur, as the soil deformation increases. Relative soil movement causes axial deformation (and, therefore, axial force) of significant value to the pipeline.

A number of investigations have been conducted, based on similar models, mainly for horizontal movement and tensile behaviour of pipelines. Among these are three well-known procedures: Newmark-Hall (1975) procedure, Kennedy et al (1977) procedure and Wang-Yeh (1985) procedure. In such cases, symmetry exists around point A, therefore there is one parameter less for the analysis.

Frequently, a specific type of ground failure in a fault zone will cause both tension and compression failures, depending on the orientation of the pipeline and its location within the zone of movement. The authors of the present paper have extended the Wang-Yeh procedure, in order to include compression phenomena. They have also included in the model the reduction of flexural stiffness of the pipe, due to severe axial forces at the large deformation area. They have come to the conclusion that, for fault movement larger than 1.0 m, flexural stiffness of the pipe can be totaly omited from the analysis, without practically affecting the accuracy of the final solution. This is valid because a large axial force reduces the values of the first and the second yield moments of the pipe, causing decrease of flexural stiffness of the pipe at any point in the large deformation region. This causes extra deformations to the pipe, which means extra reduction of the flexural stiffness. Therefore, a model has been built, by ignoring the bending stiffness of the pipe. This model is shown in Figure 1. Detail of large deformation area is shown in Figure 2. All symbols are referred to the Symbol Table, at the end of the text.

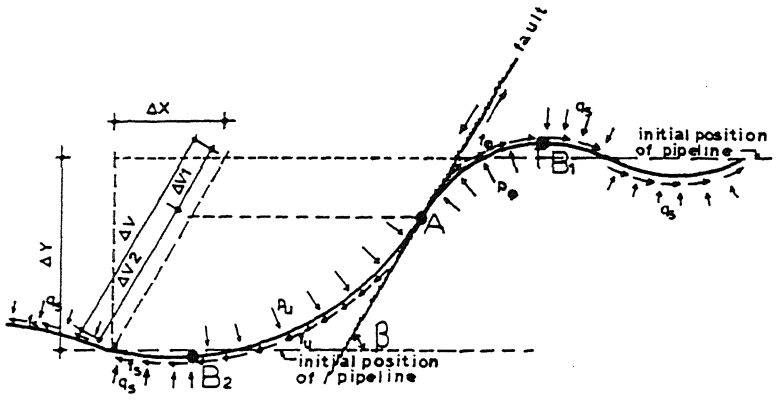

Figure 1. Model of pipeline subjected to vertical fault movement (side view).

Some related equations, from a previous paper (Vougioukas, Theodossis & Carydis (1991)) can be expressed.

For the part of the model that moves downwards:

$$\Sigma(F_x) = 0 \Longrightarrow F_{A1}\cos\alpha_1 - F_\varphi R_1 \sin\alpha_1 + P_\varphi R_1 (1 - \cos\alpha_1) - F_{B1} = 0 \quad (1)$$

$$\Sigma(F_y) = 0 \Longrightarrow -F_{A1}\sin\alpha_1 + F_\varphi R_1 (\cos\alpha_1 - 1) + P_\varphi R_1 \sin\alpha_1 = 0 \quad (2)$$

$$\Sigma(M_o) = 0 \Longrightarrow F_{A1} R_1 - F_{B1} R_1 - F_\varphi R_1^2 \alpha_1 = 0 \quad (3)$$

Similar equations can be extracted for the other part of the model, that moves upwards:

$$\Sigma(F_x) = 0 \Longrightarrow F_{A2}\cos\alpha_2 - f_u R_2 \sin\alpha_2 + P_u R_2 (1 - \cos\alpha_2) - F_{B2} = 0 \quad (4)$$

$$\Sigma(F_y) = 0 \Longrightarrow -F_{A2}\sin\alpha_2 + F_u R_2 (\cos\alpha_2 - 1) + P_u R_2 \sin\alpha_2 = 0 \quad (5)$$

$$\Sigma(M_o) = 0 \Longrightarrow F_{A2} R_2 - F_{B2} R_2 - F_u R_2^2 \alpha_2 = 0 \quad (6)$$

Balance of axial forces at section A gives:

$$F_{A1} = F_{A2} (= F_A) \quad (7)$$

Compatibility demand requires that total "geometric" (ΔG) and "permissible" (ΔP) deformations of the pipe are equal:

$$\Delta G = \Delta P \quad (8)$$

ΔG is calculated from the deformed shape of the model. ΔP is calculated from the stress-strain relations of every part of the model. Determination of ΔG and ΔP is given in detail in the same paper.

Therefore, there is a system of eight equations with eigth unknowns. It must be noted that, though the equations are extracted for fault movement causing tension to the pipeline, they are also valid for compression, provided that P_u and P_φ are given negative values, if buckling phenomena are omitted from the analysis, due to soil surrounding the pipe.

For the case of horizontal fault movement, ultimate soil resistance should be given corresponding values, equal to each other for both parts of the pipeline (symmetry around point A). In this case, Figures 1 and 2 present top view of the model.

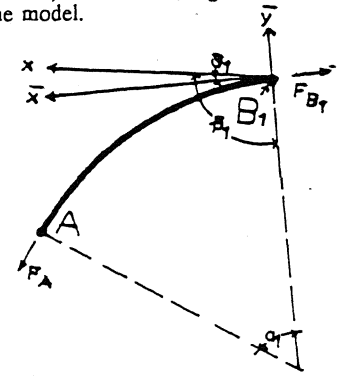

Figure 2. Detail of large deformation area of the model.

3 MATERIAL PROPERTIES

Steel X-70 has been mainly used for sample calculations in this study. Steel St-37, according to German Standards (DIN), has also been used, for comparison purposes. Stress-strain curves for X-70 and St-37 are presented in Figure 3. These curves are approximated by tri-linear curves, having the initial elastic portion up to the first yield point σ_1, then a second linear part having a much smaller slope, up to the constant ultimate yield strength σ_2. The slopes of the stress-strain curves are denoted as E_1 and E_2 for the first and the second linear portions, respectively. The first linear portion is considered as the elastic region and the second linear portion is considered as the inelastic region.

Ductility demand for the pipeline to resist fault movement is defined as the ratio $\varepsilon/\varepsilon_1$, where ε is the maximum strain at point A and ε_1 the strain corresponding to the first yield point of the material.

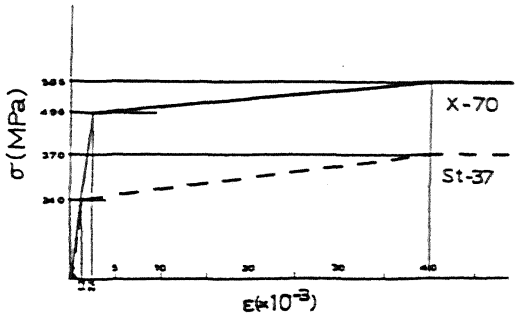

Figure 3. Stress-strain curves for steel X-70 and St-37.

4 SOIL CHARACTERISTICS

The pipe considered in our analysis is buried in a trench and backfilled with sand. The trench is wide enough, so that the properties of the sand govern pipe-soil interaction. These properties, for the sample calculations of this study, were considered as:

γ = 17.6 kN/m^3
φ = 35.0 deg
φ_p = 20.0 deg

According to Loizos (1977), the bearing capacity of the soil reaction p_φ is given by:

$p_\varphi = c N_c + \gamma_1 t N_q + 0.5\gamma_2 B N_\gamma$

In our case c=0, $\gamma_1=\gamma_2$, t=H, B=D, thus:

$p_\varphi = \gamma H N_q + 0.5 \gamma D N_\gamma$, per unit pipe area, or
$P_\varphi = \gamma H N_q D + 0.5 \gamma D^2 N_\gamma$, per unit pipe length

N_q and N_γ are, according to DIN 4017, functions of φ, (e.g. for φ = 35°, N_q = 33.3 and N_γ = 33.9).

The passive pressure of the soil is given by:

$p_u = \gamma H N_u$, per unit pipe area, or
$P_u = \gamma H N_u D$, per unit pipe lenght

N_u, according to Trautman et al (1985), is given by:

$N_u = K H/D \tan\varphi + 1 - \pi D/8H$

Away from the transition zone, the reaction of the soil to the semi-infinite pipe segments, is, according to Spangler and Handy (1973):

$q_s = 0.5 (1+k_o) + \gamma H$, per unit pipe area, or
$Q_s = 0.5 (1+k_o) D + \gamma HD$, per unit pipe length

Note that Q_s is different at each side of the pipe, due to different k_o.

Friction, anywhere on the pipe, can be found by multyipling the pressure terms by $\tan\varphi_p$. Thus:

$F_\varphi = P_\varphi \tan\varphi_p$
$F_u = P_u \tan\varphi_p$
$F_s = Q_s \tan\varphi_p$

All symbols are referred to the Symbol Table, at the end of the text.

5 ITERATIVE PROCEDURE

The given data are the soils characteristics, the geometric and material properties of the pipe and the characteristics of the movement induced by a fault: Length of relative movement ΔV (horizontal or vertical, causing tension or compression) and angle β between fault and pipe.

Though the number of the equations equals the number of the unknowns (8), equation (8) is a very complicated function, so an iterative procedure has to be used for the determination of the final solution, as follows:

F_A is given an initial value and equations (1)-(6) are used to determine the geometry of deformation (α_1, α_2, R_1, R_2) and F_{B1}, F_{B2}. Consequently, ΔV is divided in two parts ΔV_1 and ΔV_2. Then, equation (8) is used for verification of the solution. If equation (8) is not verified, F_A is given a new value, until the procedure converges. The ductility demand for the pipeline (q) to resist any given fault movement can be calculated at this point, by dividing the maximum strain that results from the analysis to the strain that corresponds to the first yield point of the material that is used for the construction of the pipeline.

A failure criterion could compare the ductility demand to the available ductility of a pipeline. Values are not, as yet, provided for this available ductility (q_a) by any regulations or specifications. Anyhow, parameters of the design must be chosen in such a way as to conclude to the lowest possible value for q.

Wang and Yeh (1985) have proposed a different failure criterion, comparing the 'response' moment to the 'resisting' moment of the pipe, after the final solution is reached. This criterion cannot be used here, as the loss of the bending resisting capacity of the pipe due to axial force is already included in the iteration procedure.

6 RESULTS AND CONCLUSIONS

After numerous parametric solutions, we came to the conclusion that, for the soil characteristics considered, the ductility demand (q) is mainly affected by six parameters:

-Type of fault movement
-Material of pipe
-Relative displacement between two parts (ΔV)
-Crossing angle (β)
-Diameter of pipe (D)
-Depth of cover (H)

Given the type of fault movement and the material of the pipe, the ductility demand can be extracted as a product of four factors, representing the influence of the last four parameters:

$$q = q_v \, q_\beta \, q_D \, q_H$$

6.1 For the case of vertical fault movement (Steel X-70)

$q_v = 0.28 \Delta V + 0.54$
$q_\beta = -0.023 \beta + 3.49$
$q_D = 1.675 D + 0.04$
$q_H = 1.365 H - 0.02$

6.2 For the case of horizontal fault movement (Steel X-70)

$q_v = 0.46 \Delta V - 0.76$
$q_\beta = -0.012 \beta + 1.59$ (for $\beta > 65°$)
and $q_\beta = -0.160 \beta + 11.30$ (for $\beta <= 65°$)
$q_D = 0.474 D + 0.21$
$q_H = 0.898 H - 0.42$

6.3 For the case of horizontal fault movement (Steel St-37)

$q_v = 0.216 \Delta V + 0.83$
$q_\beta = -0.026 \beta + 3.75$

$$q_D = 0.650\ D + 1.25$$
$$q_H = 1.236\ H + 0.16$$

In all the above relations ΔV, D and H are in meters. Angle β is in degrees. H is measured from the center of the pipe section to the top of the covering soil. Minimum value of every q_i factor (i = V, β, D, H) equals 1.00.

The relations have been extracted for the following values of parameters:

- o 1.5, 3.0, 4.5, 6.0, 7.5, 8.0, 8.5 for ΔV.
- o 60, 65, 70, 75, 80, 85, 90 for β.
- o 0.10, 0.20, 0.30, 0.60, 0.75, 0.90, 1.07, 1.20, 1.50 for D.
- o 0.2, 0.3, 0.6, 0.95, 1.2, 1.7 for (H-D/2).

At the parametric solutions performed, two of the parameters (in every possible combination) kept each time their "basic" value (the underlined ones). The proposed formulae are correlated with the actual results of the parametric solutions by a correlation coefficient from 0.85 to 0.95, depending on the case.

What can mainly be noticed, is that ductility demands are larger for the case of vertical fault movement than for the case of horizontal fault movement. That is because soil resistance to the pipe movement, due to the bearing capacity of the soil, is larger enough than resistance due to uplift reaction of the soil. The most vulnerable part of the pipeline in such a case is the "upper" part, between points A and B_1, and it is the ductility demand of this part that has been calculated.

Some geometric characteristics were found to have the following average values: $\alpha_1/\alpha_2 = 4$, $\Delta V_1/\Delta V = 0.3$

It can also be noticed that ductility demands are larger for steel St-37 than X-70. On the other hand St-37 is a more ductile material than X-70, so the behaviour of each material has to be judged separetely.

The proposed formulae have been extracted for fault movement that causes tension to the pipeline. Parametric solutions were carried out for the case of compression, using the same values of parameters as in the previous case. If buckling phenomena are not taken into account, the ductility demands are less, so the results are not of much interest.

What can be easily extracted from the formulae is that, given the type of fault and value of expected fault movement, angle β should be selected to approach 90° as much as possible. Unfortunally, angle β is not selectable for cases of vertical movement. The diameter of the pipe should be selected as small as possible. Depth of cover should be minimized as much as possible.

Another parameter that has been examined was angle of friction between soil and pipe. Though smaller values of φ_p reduce the ductility demand, this reduction, for φ_p between 15 and 30 degrees, is of relatively small value. For the proposed formulae of ductility demands (see 6.1, 6.2 and 6.3) its value is assumed to be 20 degrees.

SYMBOL TABLE

A_p	cross section of pipe
D	external diameter of pipe
E	secant modulus of elasticity of steel
E_1 (E_2)	first (second) modulus of elasticity of steel
F_{A1} (F_{A2})	axial force at point A, upper (lower) part
F_{B1} (F_{B2})	axial force at point B_1 (B_2)
F_s (f_s)	friction force, per unit length (area) of pipe, away from the transition zone
F_u (f_u)	friction force, per unit length (area) of pipe, due to the relative pipe movement upwards
F_φ (f_φ)	friction force, per unit length (area) of pipe, due to the relative pipe movement downwards
H	depth of soil covering the pipeline
k	elastic foundation spring constant
N_u	bearing capacity factor
P	axial force occuring to pipe due to fault movement
P_u (p_u)	passive pressure of soil per unit length (area) of pipe
P_φ (p_φ)	bearing capacity of the soil reaction per unit length (area) of pipe
Q_s (q_s)	reaction of the soil, away from the transition zone, per unit length (area) of pipe
R_1 (R_2)	radius of curvature of upper (lower) part
β	crossing angle
β_1, α_1, θ_1	angles,concerning geometry of upper part (Fig.2)
β_2, α_2, θ_2	angles,concerning geometry of lower part
γ	unit weight of soil
ΔG	total geometric deformation of pipe
ΔV	total relative displacement of soil surrounding the pipeline, along the fault
ΔV_1 (ΔV_2)	relative displacement of pipeline downwards (upwards), along the fault
φ	internal angle of friction of soil
φ_p	angle of friction between soil and pipe

REFERENCES

Kennedy, R.P., Chow, A.W. and Williamson, R.A. 1977. Fault movement effects on buried oil pipeline. Transportation Engineering Journal of ASCE 103: 617-633

Loizos, A.A. 1977. Soil Mechanics I, 3rd edn. National Technical University of Athens.

Newmark, N.M. and Hall, W.J. 1975. Pipeline design to resist large fault displacement. Proceedings of the U.S. National Conference on Earthquake Engineerins. Oakland. EERI.

Spangler, M.G. and Handy, R.C. 1973. Soil Engineering, 3rd edn. Intex Press. New York.

Trautmann, C.H., O'Rourke, T.D., and Kulhawy F.H. 1985. Uplift force-displacement responce of buried pipe. Journal of Geotechnical Engineering Division of ASCE, Vol 111.

Vougioukas, E.A., Theodossis, C. and Carydis, P.G. 1991. Seismic analysis of buried pipelines subjected to vertical fault movement. Technical Council on Lifeline Earthquake Engineering (TCLEE), Monograph No 4.

Wang, R.R.-L. and Yeh Y.-H. 1985. A refined seismic analysis and design of buried pipeline for fault movement. Journal of Earthquake Engineering and Structural Dynamics, Vol 13.

ACKNOWLEDGEMENT

The authors want to thank Mr C.V. Theodossis for his contribution to the present paper.

Earthquake Engineering, Tenth World Conference © 1992 Balkema, Rotterdam. ISBN 90 5410 060 5

Interpretation of high pressure pipeline damage by liquefaction-induced ground movements

F. Miura
Yamaguchi University, Ube, Japan

T. D. O'Rourke
Cornell University, Ithaca, USA

M. Hamada
Tokai University, Shimizu, Japan

ABSTRACT: During the 1971 San Fernando earthquake, large ground deformations occurred at the Joseph Johnson Filtration Plant along the west side of the Upper Van Norman Reservoir. Recent analyses of aerial photographs taken before and after the earthquake have provided a comprehensive view of lateral and vertical ground movements at the site. Most pipelines in the utility corridor at the site were not damaged, but some pipelines were damaged by the ground movements. The object of this study is to show by numerical analyses why some of the pipelines were damaged while others were not. The analyses showed that for in-situ stress and frictional resistance pertaining to medium dense sand, almost the same magnitudes of stress as that of the yield stress were estimated at a location where tensile failure occurred for Grade-B steel pipelines. But lower stress levels were estimated for x-52 steel pipelines, which sustained the ground movements.

1 AIR PHOTO AND OPTICAL SURVEY MEASUREMENTS

Photogrammetric analyses were performed on high quality air photographs taken before and after the 1971 San Fernando earthquake for the west side of the Upper Van Norman Reservoir area (O'Rourke et al. 1989), where large ground displacements occurred during the earthquake. The interpretation process has been discussed in several publications

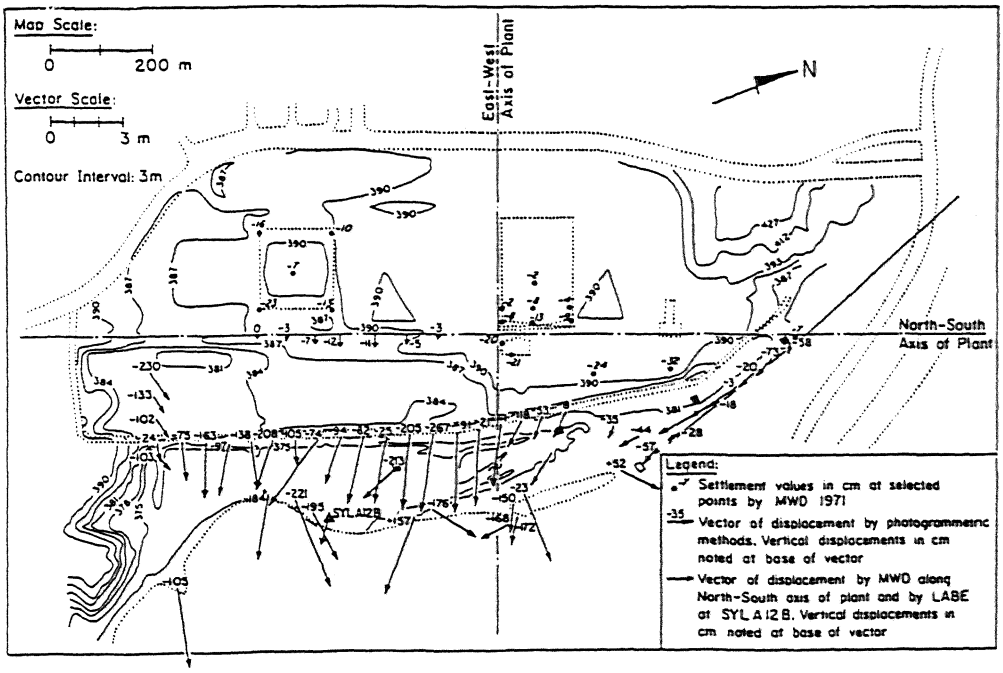

Figure 1. Displacements determined from air photo analyses and optical surveys.

(e.g. Hamada et al. 1985). The results of these analyses are shown in Figure 1 as vectors of horizontal movement and measurements of settlement and heave. Measurement accuracy is approximately 10 to 20 mm for lateral movement and settlement. Optical survey measurements performed by the Metropolitan Water District of Southern California (MWD) are also shown at various locations. For example, lateral offsets surveyed along the north-south plant axis and settlements at several key structures are included in the figure.

The air photo analyses show lateral ground movements along the utility corridor, typically 2 to 3 m, in an easterly direction toward the reservoir. At the eastern terminus of the Outlet Conduit, air photo measurements show lateral soil movements of 1.3 to 2.2 m, which agree reasonably well with the total cumulative movement measured on the ground at this location.

2 PIPELINE DAMAGE AT THE UPPER VAN NORMAN RESERVOIR

Figure 2 shows a plan view of the area west of the Upper Van Norman Reservoir on which are superimposed ground ruptures associated with liquefaction-induced ground failures in this locality. The locations of pipeline damage were determined from repair records provided through the courtesy of the Los Angeles Department of Water and Power (LADWP) and the Getty Oil Company. The information in the repair records was supplemented by discussions with utility personnel. The locations of pipeline repairs are designated by solid triangles in the figure. Table 1 summarizes information about the pipelines and includes dimensions, installation date, composition, joint type, coating, depth of soil cover, and nominal operating pressure at the time of the earthquake. The outside diameter (O.D.) and wall thickness for each pipe are listed in the column headed dimension. Each pipeline is numbered for the purpose of referencing and corresponds to the numbers used in the Typical Section in Figure 2. In general, the pipelines were buried in medium dense and silty sands above the water table. Transmission pipelines for natural gas, liquid fuel, and water were involved, representing different dimensions, joint design, operating pressures, welding practices, and age. Pipelines operated by the Los Angeles Department of Water and Power and the Southern California Gas Company are prefaced by DWP and SCG, respectively.

Most pipelines in the utility corridor were not damaged, including the three lines operated by the Southern California Gas Company and one operated by the Mobil Oil Corporation (pipelines 6a, 6b, 7, and 9 in Table 1). Some gas pipelines were cut and rewelded after the earthquake, principally to relieve residual stresses and make adjustment for deformations caused by the ground movements. Pipeline 8, operated by the Getty

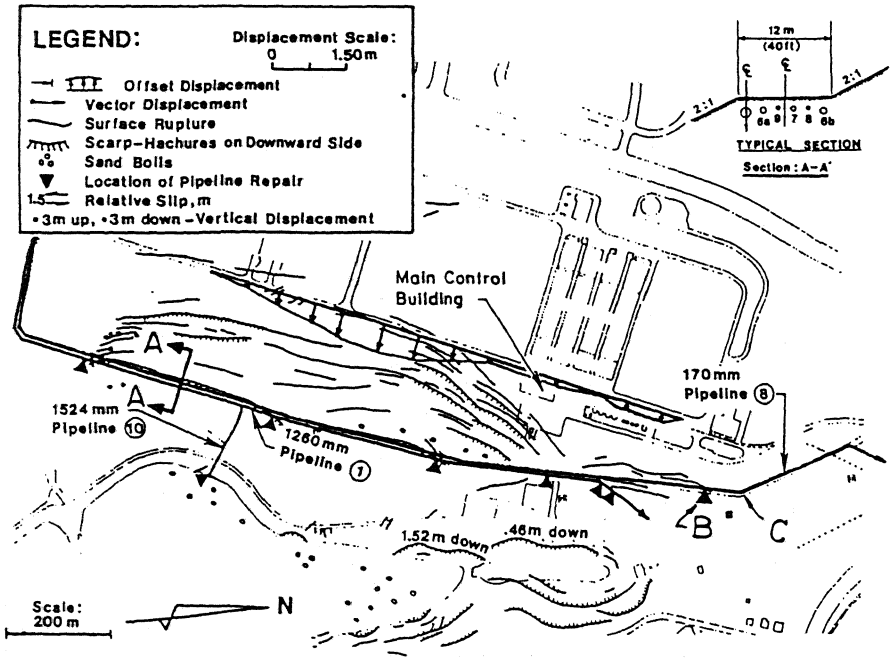

Figure 2. Locations of pipeline repairs, west side of the Upper Van Norman Reservoir.

Table 1. Information summary for pipelines affected by ground movements.

Number	Pipeline	Dimensions	Installation Date	Composition	Joints	Cbating	Depth of Cover	Operatinq Pressure
1	DWP Granada Trunk Line	1260mm O.D.; 6.4mm wall thickness	1967	Steel, ASTM A-283 Grade C	Arc welded slip joints on 9m centers	Cement, 25.4mm thick	1.0m	0.7-1.4MPa
6a, 6b	SCG Lines 3000 & 3003	760mm O.D.; 9.5mm wall thickness	1966	Steel, X-52 Grade	Arc welded girth joints on 12m centers	Asphalt, fiberglass, asbestos felt	1.0-1.2m	1.4-3.2MPa
7	SCG Line 120	560mm O.D.; 7.2mm wall thickness	1966	Steel, X-52 Grade	Arc welded girth joints on 12m centers	Asphalt, fiberglas and asbestos felt	1.0-1.2m	1.4MPa
8	Getty Oil Company Line	170mm O.D.; 7.2 mm wall thickness	1966	Steel, API Grade B	Arc welded girth joints on 12m centers	Coal tar enamel & fiberglas	1.0-1.2m	0.7-1.0MPa
9	Mobil Oil Corporation Line	400mm O.D.; 7.9mm wall thickness	1966 1969	Steel, X-52 Grade	Arc welded girth joints on 12m centers	Coal tar enamel & fiberglas	1.0-1.2m	No internal pressure at time of earthquake
10	DWP Plant Connection	1524mm O.D.; 9.5mm wall thickness	1970	Steel, ASTM A-283 Grade C	Arc welded slip joints on 9m centers	0.6m thick reinforced concrete encasement	2.0m	No internal pressure at time of earthquake

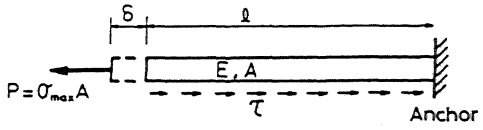

Figure 3. A model of a pipe for numerical analyses.

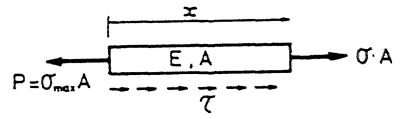

Figure 4. The equeliburium condition.

Oil Company, failed in tension across a weld at the northern boundary of the landslide area (Point B in Figure 2). The analyses for pipeline 8 are discussed in the following chapter. Detailed discussion of the damage at other points is given by O'Rourke et al. (1990).

3 NUMERICAL ANALYSES

In order to interpret the reason why some of the pipelines were damaged at point B in Figure 2, while others were not damaged, numerical analyses were performed to evaluate the response of the pipelines to ground movements. The pipelines were assumed to be anchored at location C in Figure 2, where the pipelines bend to the northwest. Based on this assumption, the model shown in Figure 3 was empoyed to estimate the maximum tensile stress, σ_{max}, in the pipelines at location B in Figure 2, where tensile failure was observed for pipeline 8. The magnitude of δ, which is the elongation of the pipe at the length, ℓ, was obtained by assuming that the pipelines south of location C were deformed in accordance with the ground displacements shown in Figure 1.

3.1 The relationship between δ and σ_{max}

The equilibrium condition of part of a pipeline of which length is x is given by (see Figure 4);

$$\sigma = \sigma_{max} - \frac{\tau}{A} x \qquad (1)$$

where, σ = stress at x, σ_{max} = the maximum stress at the end of the pipe, τ = shearing resistance along the pipe per unit length, A = area of cross-section of the pipe.

The shearing resistance, τ, is assumed to be a function of the unit weight of soil, γ, the coefficient of earth pressure at rest, Ko, the depth of the pipe below the ground surface, H, the outer diameter of the pipe, D, and the friction angle between the pipe and soil, ϕ, and is given by;

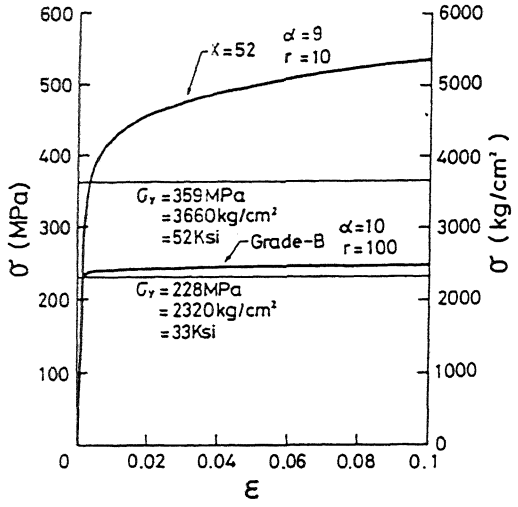

Figure 5. The stress-strain curves for analyzed pipes.

$$\tau = \frac{1+Ko}{2}\gamma H \tan\phi\, \pi D \qquad (2)$$

The relationship between stress and strain induced in the pipe is expressed by Equation (3) by assuming the Ramberg-Osgood stress-strain relationship;

$$\varepsilon = \frac{\sigma}{E}\left\{1 + \frac{\alpha}{1+r}\left(\frac{\sigma}{\sigma_y}\right)^r\right\} \qquad (3)$$

where, ε = strain, σ_y = the yield stress, and α and r are dimensionless parameters.

Substituting Equation(1) into (3) we get the strain at x;

$$\varepsilon = \frac{\sigma_{max} - \frac{\tau}{A}x}{E}\left\{1 + \frac{\alpha}{1+r}\left(\frac{\sigma_{max} - \frac{\tau}{A}x}{\sigma_y}\right)^r\right\} \qquad (4)$$

The elongation, δ, is obtained by integrating the strain given by Equation (4) from 0 to l with respect to x, as follows;

$$\delta = \int_0^l \varepsilon\, dx$$

$$= \frac{l}{E}\left(\sigma_{max} - \frac{\tau}{2A}l\right) - \frac{\alpha A}{E(1+r)(2+r)\tau\sigma_y^r}$$

$$\cdot\left\{\left(\sigma_{max} - \frac{\tau}{A}l\right)^{r+2} - \sigma_{max}^{r+2}\right\} \qquad (5)$$

By assuming that the pipelines were deformed in accordance with the ground displacements, the magnitude of elongation at l = 75 m was estimated to be 0.0561 m.

3.2 Stress-strain relationships in the pipes

It is necessary to determine the parameters α and r for the analyzed pipes, Grade-B and X-52 steels. The stress-strain curves shown in Figure 5 were used for these pipes. The parameters were α = 10 and r = 100 for the Grade-B steel and α = 9 and r = 10 for the X-52 steel.

The yield stresses of the Grade-B and the X-52 steels are 228 Mpa (2320 kg/cm2, 33 ksi) and 359 Mpa (3660 kg/cm2, 52 ksi), respectively. After yielding, the Grade-B steel has a very flat slope, but the X-52 steel has a steep slope.

3.3 Results

The length, l, was 75 m and the elongation, δ, was 0.0561 m. The depth of the pipes, H, was determined from Table 1, and the unit weight of soil was assumed to be 1.8 g/cm3. For the parameters Ko and ϕ, the values of 0.5, 0.75, 1.0 and 30°, 35°, 40° were assumed.

The maximum tensile stresses normalized by the yield stress, σ_{max}/σ_y obtained from Equation (6) are shown in Figure 6. This figure shows that the stress ratios for the Grade-B steel are almost 1, but much smaller than 1 for the X-52 steel. This means that these stresses are nominally sufficient to yield the Grade-B steel but not the X-52 steel. If the Grade-B steel in pipeline 8 had a relatively flat slope in the post yield portion of its stress-strain curve, as shown in Figure 5, then such stress would be sufficient to rupture the line. In contrast, the X-52 steel in pipelines 6a, 6b, 7 and 9 had both sufficient reserve against yield and ductility to sustain the ground deformation imposed on them. This means that the post-yield slope in the stress-strain curve, as well as the magnitude of the yield stress is very important, when a buried pipeline is subjected to large ground deformation.

4 CONCLUSIONS

The 1971 San Fernando earthquake provides the opportunity to relate large ground deformation, various soil conditions, and the response of buried pipelines of different size, composition, and age. Of particular interest is the area west of the Upper Van Norman Reservoir, where liquefaction-induced soil movements subjected six different pipelines to virtually the same pattern of gro-

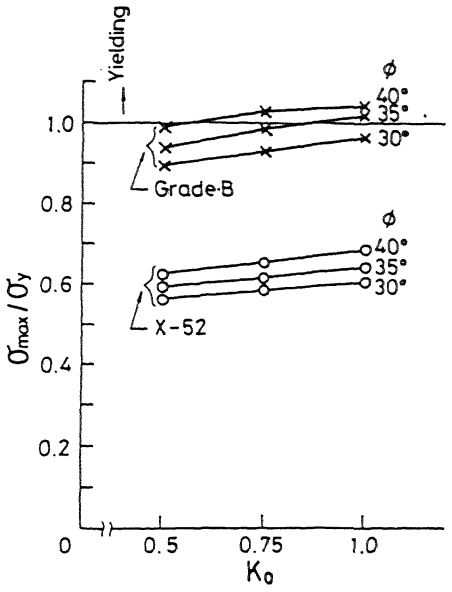

Figure 6. The normalized maximum stresses induced in the analyzed pipes.

und displacement.

A reliable record of pipeline performance involves both failed pipelines and those which were able to sustain large differential movement. In order to understand this phenomena, numerical analyses were performed.

The results revealed that the stresses induced in the pipelines were nominally sufficient to yield the Grade-B steel, but not the X-52 steel. Steels with relatively low yield stress, particularly those manufactured over 20 to 30 years ago, such as the Grade-B steel, may be characterized by a relatively flat slope when tensile stress is plotted with respect to strain in the post yield range of axial deformation. In contrast, high stress steels with steeper post-yield slopes, such as the X-52 steel are able to accommodate ground movement even though the magnitude maybe several meters. This shows that the post-yield slope is critically important for the level of maximum strain in the steel as well as the yield stress when a buried pipeline is subjected to tensile ground movements.

REFERENCES

Hamada, M., S. Yasuda, R. Isoyama, and K. Emoto 1985. Study of liquefaction-induced permanent ground displacements. Association for the Development of Earthquake Prediction, Tokyo.

O'Rourke, T.D., B.L. Roth, & M. Hamada 1989. A case study of large ground deformation during the 1971 San Fernando earthquake. 2nd U.S.-Japan workshop on liquefaction, large ground deformation, and their effects on lifeline facilities. 67-81.

O'Rourke, T.D. & M.S. Tawfik 1983. Effects of lateral spreading on buried pipelines during the 1971 San Fernando earthquake. PVP-Vol.77, ASME. New York. 124-132.

O'Rourke, T.D., B.L. Roth, F. Miura, and M. Hamada 1990. Case history of high pressure pipeline response to liquefaction-induced ground movements. Proc. of Fourth U.S. National Conf. on Earthquake Eng. Palm Springs. 955-964.